Supplemental Figures and Tables

Supplemental Table 1. Primers for qPCR

Gene	Forward Primer	Reverse Primer
Il-6	5'-CAGACTCGCGCCTCTAAGGAGT-3'	5'-GATAGCCGATCCGTCGAA-3'
Mcp1	5'-GATAGCCGATCCGTCGAA-3'	5′-GCTACCACAACATCTGGACATT-3′
Mmp9	5′-AACCAATGATGCTGGGTTCAC-3′	5'-GCGCCGACTCAGAGGTGT-3'
Gapdh	5′-TCGATATTGAGCGTCCAACCT-3′	5′-CAAAGGCACGTTTGGCATACA-3′
Dusp15	5′-CCTGGACTCTACCTTGGAAAC-3′	5′-GTGGATAAAGTGGACGCATTC-3′
mtHsp70	5′-AGACCACTGTTCAGATGACCATGG -3′	5′- TTAGAAGTCTGGAGCGGTCAATGC -3′
Lonp1	5′-AGGATCACCCTGAGTTCCCAGTT-3′	5′-ACCACCTATAGCAGGTGCGAA-3′
Hsp10	5′-GGCCCGAGTTCAGAGTCC-3′	5′-TGTCAAAGAGCGGAAGAAACTT-3′
Clpp	5′-CACAGACATCGCCATCCA-3′	5′-TCCCTCTCCATTGCTGACTC-3′
mtDNAj	5′-AGTCACCCACACAAGCACTG-3′	5′-CCAGCCTCTCGCCTATCC-3′
Atf5	5′-CTGGCTCCCTATGAGGTCCTTG-3′	5′-GAGCTGTGAAATCAACTCGCTCAG-3′

Supplemental Table 2. Antibody information

Name	Catalogue number	Dilution factor
Dusp15	Thermo Fisher Scientific Inc., #PA5-109666	1:1000
mtHsp70	Thermo Fisher Scientific Inc., #MA3-028	1:1000
Collagen I	Abcam, #ab270993	1:1000
Collagen III	Abcam, #ab184993	1:1000
TGFβ	Abcam, #ab215715	1:1000
GAPDH	Santa Cruz Biotechnology, # sc-373841	1:1000

Supplemental Figures

Supplemental Figure 1. Schematic of the experimental design for the mouse study.

To model DCM, we used a HFD combined with low-dose streptozotocin (STZ) injections, as previously described with modifications. Briefly, C57BL/6J mice were fed an HFD (Research Diets, D12492) for 8 weeks to induce insulin resistance, followed by intraperitoneal administration of STZ (35 mg/kg; Sigma-Aldrich, S0130) dissolved in sodium citrate buffer (50 mmol/L, pH 4.5) for three consecutive

days. The mice continued on the HFD for an additional 16 weeks. Control mice received a standard normal control diet (NCD, Research Diets, D12450J) and citrate buffer injections.

Supplemental Figure 1

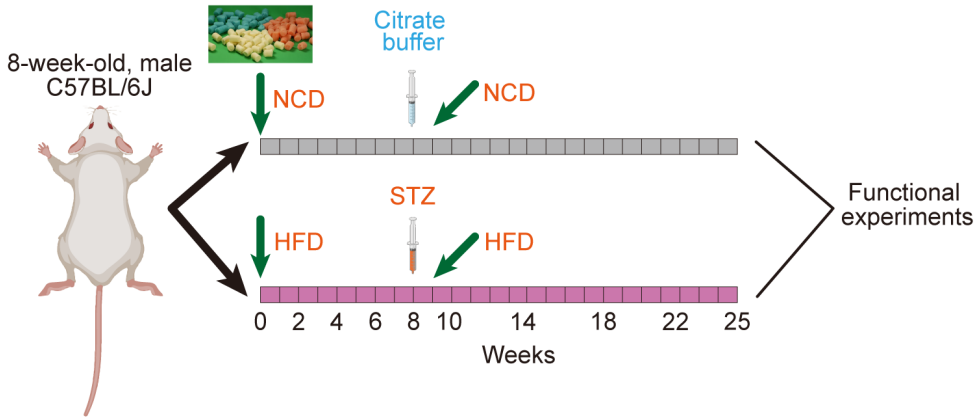

Supplemental Figure 2. *Dusp15* deficiency excerbates hyperglycemia-induced myocardial dysfunction in diabetic cardiomyopathy.

In vivo, cardiomyocyte-specific Dusp15 knockout (*Dusp15*^{Cko}) and *Dusp15*$^{f/f}$ mice were subjected to a high-fat diet (HFD) for 8 weeks followed by intraperitoneal injections of streptozotocin (STZ, 35 mg/kg) for three consecutive days, with continued HFD feeding for another 16 weeks. Control mice were fed a normal control diet (NCD) and received citrate buffer injections.

(A) Echocardiographic analysis of heart function in *Dusp15*^{Cko} and *Dusp15*$^{f/f}$ mice, evaluating parameters including left ventricular ejection fraction (LVEF), fractional shortening (FS), left ventricular systolic dimension (LVSd), ratio of early to late transmitral flow velocities (E/A), ratio of diastolic mitral annulus velocities (e'/a'), ratio of mitral peak velocity of early filling to early diastolic mitral annular velocity (E/e'), and left ventricular diastolic dimension (LVDd).

(B) Assessment of contractile properties in acutely isolated ventricular cardiomyocytes, including resting cell length, peak shortening (PS), maximal velocity of shortening (+dL/dt), time-to-peak shortening (TPS), maximal velocity of relengthening (-dL/dt), and time-to-90% relengthening (TR90). All data are presented as mean ± SD. In each group, six animals or six independent cell isolations were used. Each experiment was conducted with three replicates.

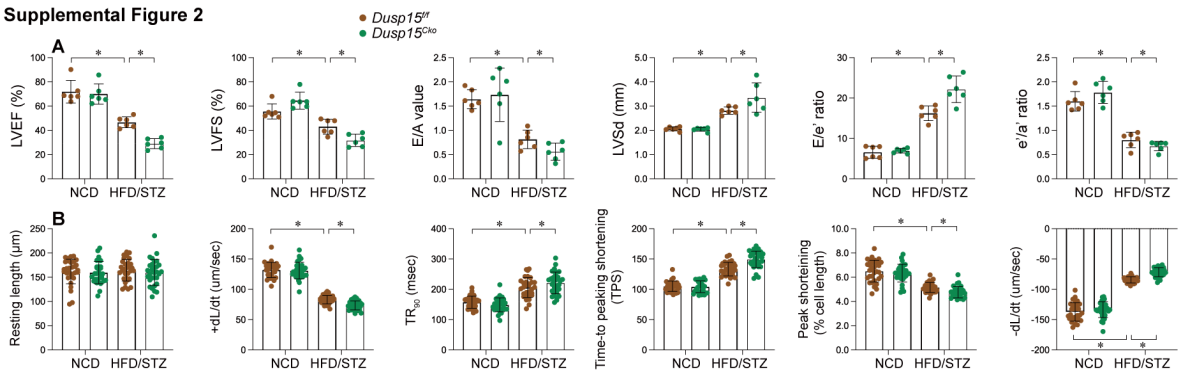

Supplemental Figure 3. *Dusp15* ablation excerbates hyperglycemia-induced myocardial structural disorder in diabetic cardiomyopathy.

In vivo, cardiomyocytes-specific *Dusp15* knockout (*Dusp15*^{Cko}) and *Dusp15*$^{f/f}$ mice were subjected to a high-fat diet (HFD) for 8 weeks followed by intraperitoneal injections of streptozotocin (STZ, 35 mg/kg) for three consecutive days, with continued HFD feeding for another 16 weeks. Control mice were fed a normal control diet (NCD) and received citrate buffer injections.

(A) Representative images of hematoxylin and eosin (H&E)-stained heart tissue sections showing myocardial structure in *Dusp15*^{Cko} and *Dusp15*$^{f/f}$ mice under diabetic conditions.

(B) Representative images of Masson-stained heart tissue sections showing myocardial structure in *Dusp15*^{Cko} and *Dusp15*$^{f/f}$ mice.

(C) Representative images of Sirius Red-stained heart tissue sections showing myocardial structure in *Dusp15*^{Cko} and *Dusp15*$^{f/f}$ mice.

(D) Quantification of myocardial fibrosis was performed using Masson staining to evaluate the extent of collagen deposition in cardiac tissues.

(E-G) Proteins were isolated from heart tissues and the expression of collagen I, collagen III, and TGFβ were measured via western blots.

(H) ELISA was used to analyze the activity of MMP9 in heart tissues.

(I-K) RNA was isolated from heart tissues and then the transcription of MCP1, IL-6 and TNFα were measured via qPCR.

(L) Representative transmission electron microscopy (TEM) images of cardiac ultra-structure from *Dusp15*^{Cko} and *Dusp15*$^{f/f}$ mice under normal and diabetic conditions.

All data are presented as mean ± SD. In each group, six animals or six independent cell isolations were used. Each experiment was conducted with three replicates.

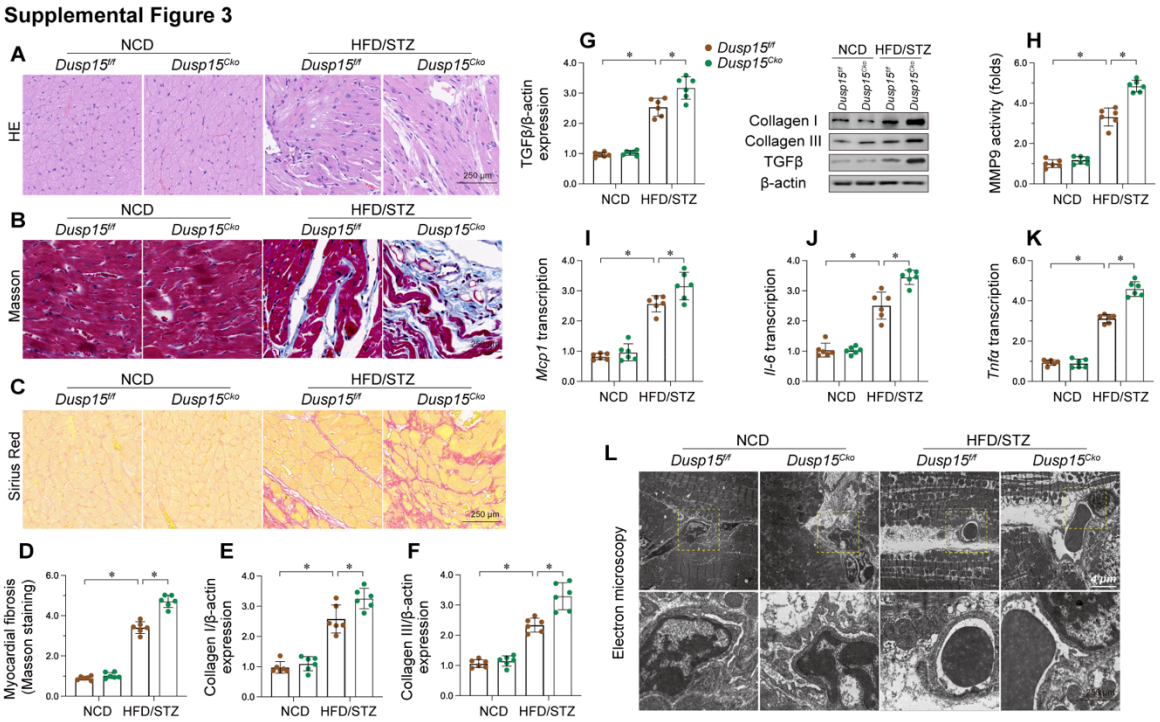

Supplemental Figure 4. Dusp15 find-tunes mito-UPR in ventricular cardiomyocytes during DCM.

(A) Single-cell RNA-seq analysis was performed using the Genome Sequence Archive in BIG Data Center (accession code CRA007245), which contains the nuclear fractions of all cardiac cells single-cell RNA-seq data from 6 healthy controls (16,490 cells) and 6 HFD/STZ-induced diabetic mice (16,095 cells). All ventricular cardiomyocytes in the DCM group were stratified into high Dusp15 (hiDusp15) and low Dusp15 (loDusp15) subgroups based on the median expression of Dusp15

(B) GO enrichment analyses of Biological Process, Cellular Component, and Molecular Function categories was performed to highligh the altered pathways in DCM.

(C) KEGG analysis demonstrated significant enrichment of pathways in diabetic mice.

(D) Gene Set Enrichment Analysis (GSEA) of mito-UPR-related pathways.

(E-F) Single-sample GSEA (ssGSEA) scoring of mtUPR activity in ventricular cardiomyocytes. High Dusp15 expression closely aligned with elevated mtUPR activity.

(G) Evaluation of UPR activity across all cardiac cell subpopulations from single-cell data.

(H) In vivo, cardiomyocyte-specific *Dusp15* knockout (*Dusp15*^{Cko}) and wild-type *Dusp15*$^{f/f}$ mice were subjected to a high-fat diet (HFD) for 8 weeks followed by intraperitoneal injections of streptozotocin (STZ, 35 mg/kg) for three consecutive days, with continued HFD feeding for another 16 weeks. Control mice were fed a normal control diet (NCD) and received citrate buffer injections. Validation of mito-UPR activity in vivo was performed using qPCR in *Dusp15*^{Cko} and *Dusp15*$^{f/f}$ mice.

All data are presented as mean ± SD. In each group, six animals or six independent cell isolations were used. Each experiment was conducted with three replicates.

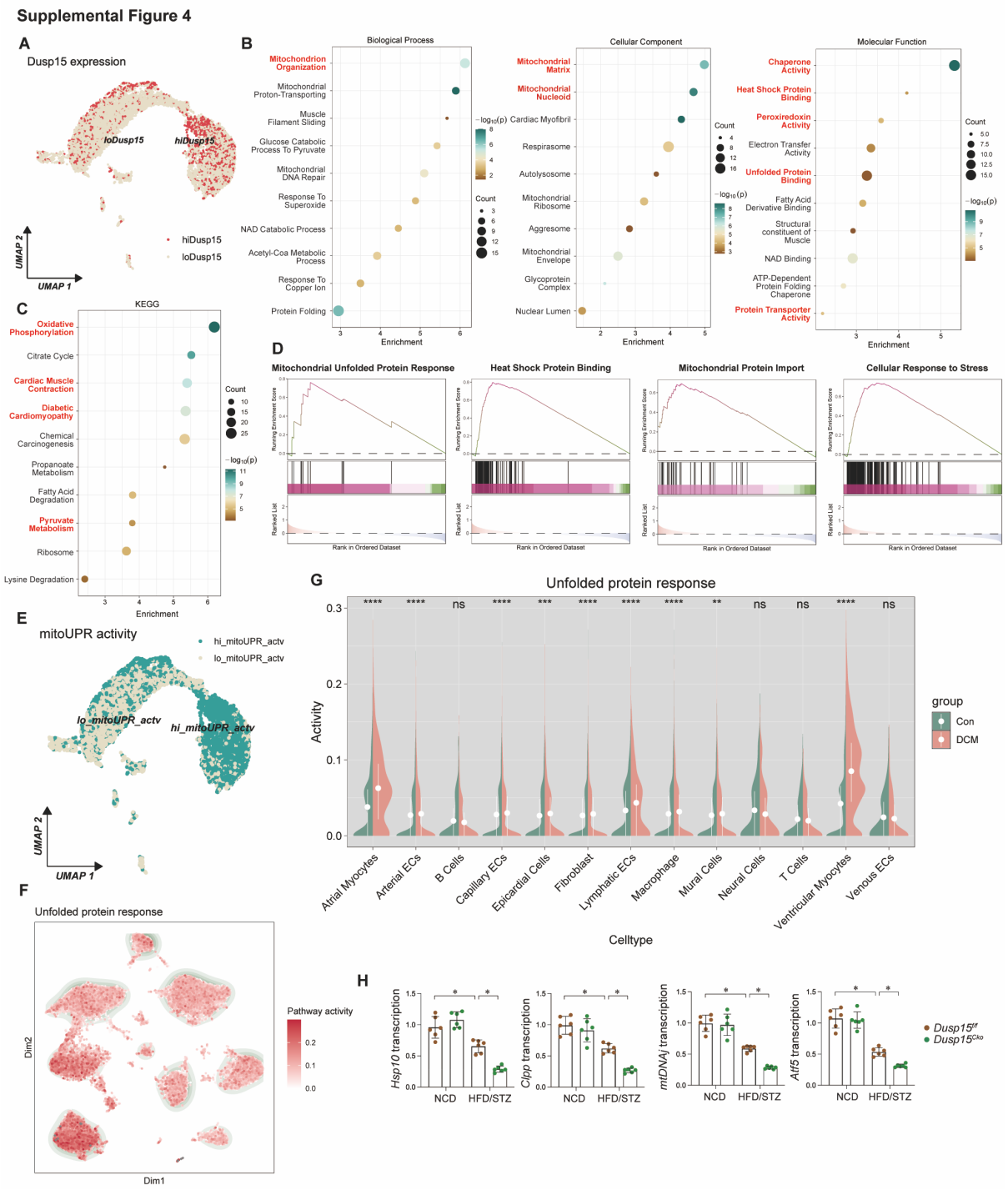

Supplemental Figure 5. Assessment of mitochondrial function and oxidative stress in response to *Dusp15* overexpresison.

In vivo, HL-1 cells were incubated with high glucose (HG, 30 mmol/L) for 48 hrs to induce hyperglycemic stress. HL-1 cells cultured under normal glucose (NG, 5.5 mmol/L) medium was used as the control group. Cells were treated with lentiviral vectors for *Dusp15* overexpression (LV-Dusp15) or control vectors.

(A) ΔΨm was determined using JC-1 staining, where the fluorescence shift between red (aggregates) and green (monomers) indicates changes in membrane potential.

(B) Quantification of the red/green fluorescence intensity ratio to assess ΔΨm changes.

(C) Mitochondrial reactive oxygen species (mtROS) were measured using MitoSOX™ Red fluorescence. HL-1 cells were subjected to HG conditions with or without LV-Dusp15 treatment.

(D) Fluorescence intensity of mtROS was quantified using confocal microscopy and ImageJ software.

All data are presented as mean ± SD. In each group, six animals or six independent cell isolations were used. Each experiment was conducted with three replicates.

Supplemental Figure 5

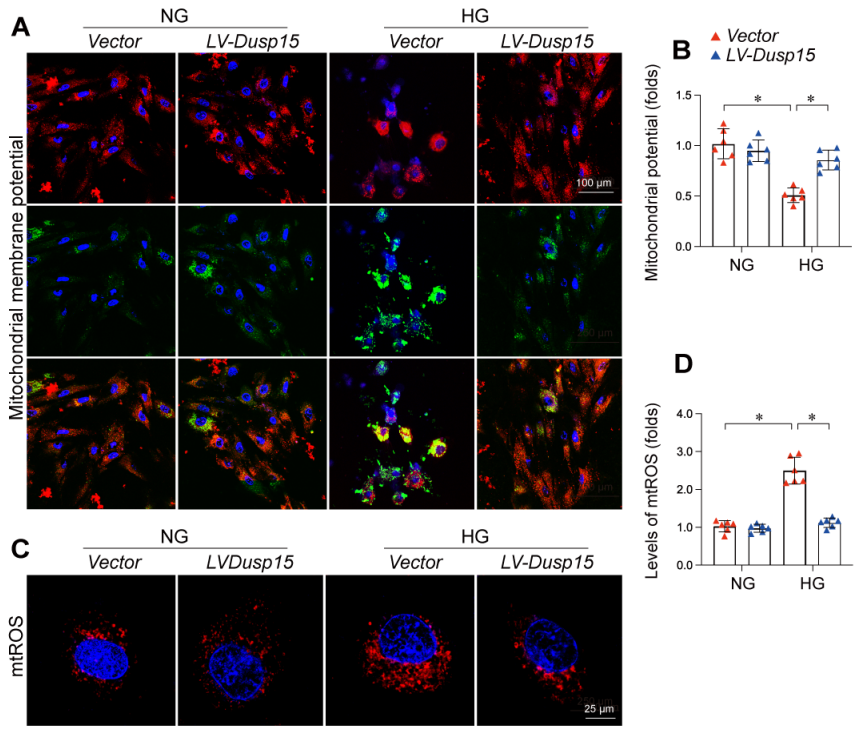

Supplemental Figure 6. Assessment of mitochondrial function and oxidative stress in response to mito-UPR inhibition.

In vivo, HL-1 cells were incubated with high glucose (HG, 30 mmol/L) for 48 hrs to induce hyperglycemic stress. HL-1 cells cultured under normal glucose (NG, 5.5 mmol/L) medium was used as the control group. Cells were treated with lentiviral vectors for *Dusp15* overexpression (LV-Dusp15) or control vectors. To inhibit the activity of mito-UPR, HL-1 cells were pretreated with DCEM1 (20 μM) 1 hrs before HG treatment.

(A) ΔΨm was determined using JC-1 staining, where the fluorescence shift between red (aggregates) and green (monomers) indicates changes in membrane potential.

(B) Quantification of the red/green fluorescence intensity ratio to assess ΔΨm changes.

(C) Mitochondrial reactive oxygen species (mtROS) were measured using MitoSOX™ Red fluorescence. HL-1 cells were subjected to HG conditions with or without LV-Dusp15 treatment.
(D) Fluorescence intensity of mtROS was quantified using confocal microscopy and ImageJ software.
All data are presented as mean ± SD. In each group, six animals or six independent cell isolations were used. Each experiment was conducted with three replicates.

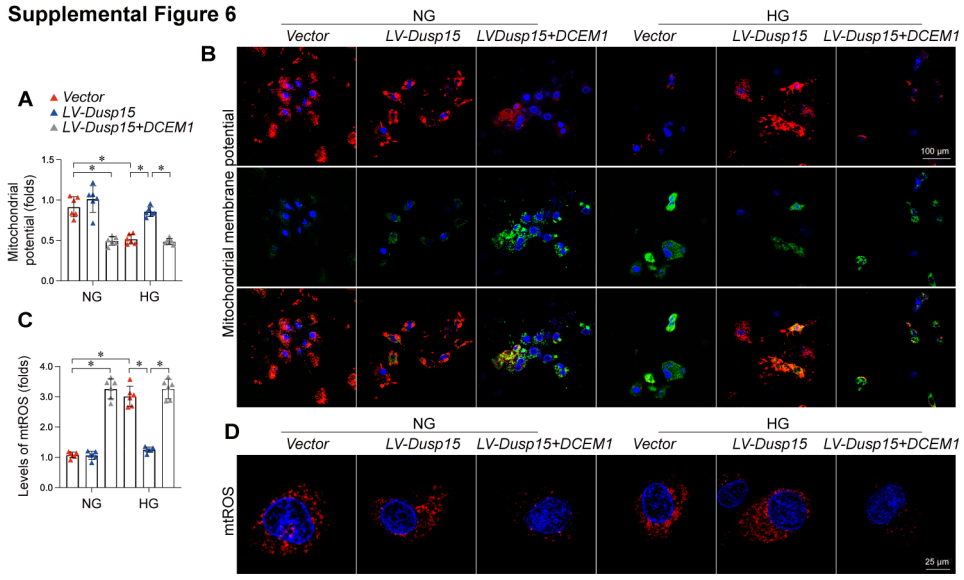

Supplemental Figure 7. The alterations of Dusp15 and mtHsp70 in DCM.

In vivo, *Dusp15* transgenic (*Dusp15*^{Tg}) and wild-type (*WT*) mice were subjected to a high-fat diet (HFD) for 8 weeks followed by intraperitoneal injections of streptozotocin (STZ, 35 mg/kg) for three consecutive days, with continued HFD feeding for another 16 weeks. Control mice were fed a normal control diet (NCD) and received citrate buffer injections. *In vivo*, HL-1 cells were incubated with high glucose (HG, 30 mmol/L) for 48 hrs to induce hyperglycemic stress. HL-1 cells cultured under normal glucose (NG, 5.5 mmol/L) medium was used as the control group. Cells were treated with lentiviral vectors for Dusp15 overexpression (LV-Dusp15) or control vectors. Besides, HL-1 cardiomyocytes were transfected with shRNAs targeting mtHsp70 or a scrambled control.
(A-B) Quantitative real-time PCR was performed on extracted RNA to assess the transcription levels of Lonp1 and mtHsp70.
(C-F) qPCR assay was used to evaluate the changes of mito-UPR-related markers.
All data are presented as mean ± SD. In each group, six animals or six independent cell isolations were used. Each experiment was conducted with three replicates.

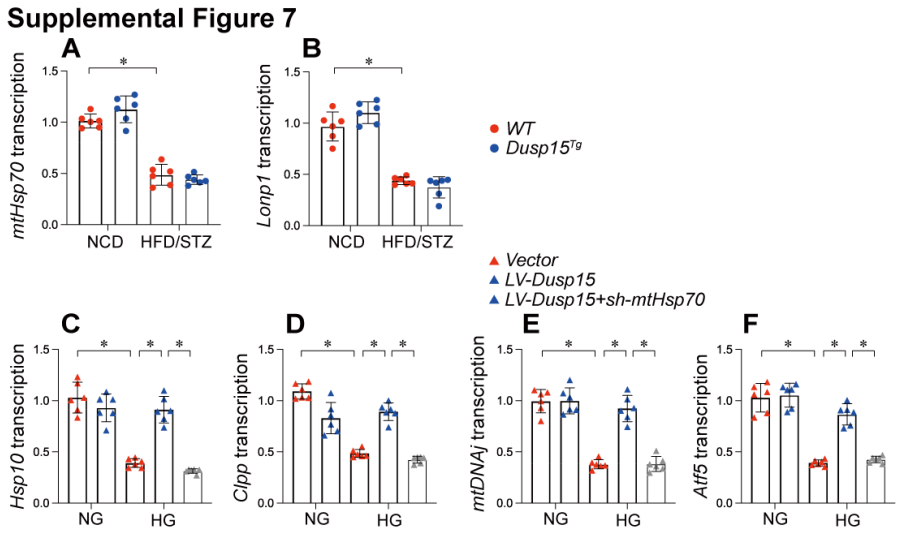

Supplemental Figure 8. Dusp15 binds to mtHsp70.

(A) HL-1 cells were transfected with different domain deletion Dusp15 mutants before HG treatment. Then, western blots were used to figure out the expression of mtHsp70.

(B) Cells were treated with lentiviral vectors for *Dusp15* overexpression (LV-Dusp15) or control vectors. Then, sodium orthovanadate (SO) was applied to incubate with HL-1 cells to inhibit the Dusp15 phosphatase activity. Western blots were used to figure out the expression of mtHsp70.

(C) HL-1 cells were transfected with Myc-Dusp15 and then treated with SO to inhibit the Dusp15 phosphatase activity. Then, sample from HL-1 cells were lysed, and the interaction between exogenous Dusp15 and mtHSP70 was assessed by Co-IP.

All data are presented as mean ± SD. In each group, six animals or six independent cell isolations were used. Each experiment was conducted with three replicates.

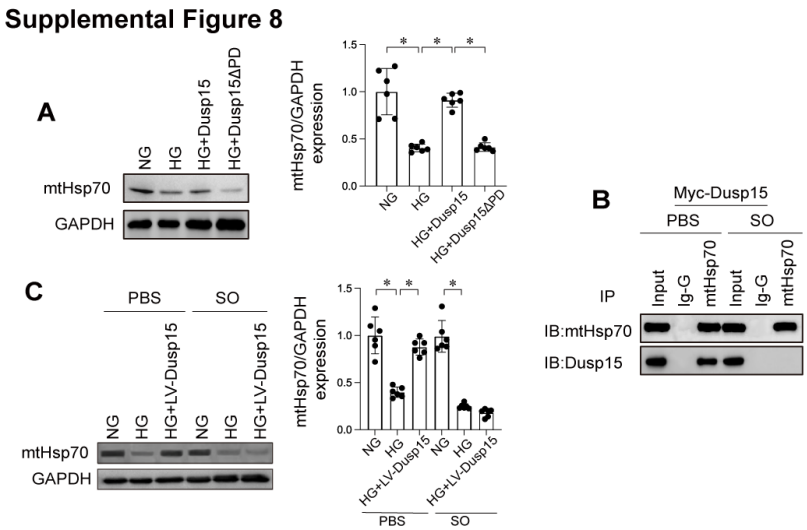

Supplemental Figure 9. *mtHsp70* knockout excerbates hyperglycemia-induced myocardial dysfunction and mitochondrial abnormalities.

In vivo, cardiomyocytes-specific *mtHsp70* knockout (*mtHsp70*^{Cko}) and *mtHsp70*$^{f/f}$ mice were subjected to a high-fat diet (HFD) for 8 weeks followed by intraperitoneal injections of streptozotocin (STZ, 35 mg/kg) for three consecutive days, with continued HFD feeding for another 16 weeks. Control mice were fed a normal control diet (NCD) and received citrate buffer injections. *In vivo*, HL-1 cells were incubated with high glucose (HG, 30 mmol/L) for 48 hrs to induce hyperglycemic stress. HL-1 cells cultured under normal glucose (NG, 5.5 mmol/L) medium was used as the control group. Cells were treated with shRNA against *mtHsp70* to knockdown the expression of mtHsp70.

(A) Echocardiographic analysis of heart function in *mtHsp70*^{Cko} and *mtHsp70*$^{f/f}$ mice, evaluating parameters including left ventricular ejection fraction (LVEF), fractional shortening (FS), left ventricular systolic dimension (LVSd), ratio of early to late transmitral flow velocities (E/A), ratio of diastolic mitral annulus velocities (e'/a'), ratio of mitral peak velocity of early filling to early diastolic mitral annular velocity (E/e'), and left ventricular diastolic dimension (LVDd).

(B) Assessment of contractile properties in acutely isolated ventricular cardiomyocytes, including resting cell length, peak shortening (PS), maximal velocity of shortening (+dL/dt), time-to-peak shortening (TPS), maximal velocity of relengthening (-dL/dt), and time-to-90% relengthening (TR90).

(C-E) Representative histopathological images from diabetic *mtHsp70*^{Cko} and *mtHsp70*$^{f/f}$ mice treated with or without DCEM1, showing myocardial disarray (H&E staining) and fibrosis (Masson trichrome and Sirius Red staining).

(F) Quantification of myocardial fibrosis was performed using Masson staining to evaluate the extent of collagen deposition in cardiac tissues.

(G) ELISA was used to analyze the activity of MMP9 in heart tissues.

(H-J) RNA was isolated from heart tissues and then the transcription of MCP1, IL-6 and TNFα were measured via qPCR.

(K) ΔΨm was determined using JC-1 staining, where the fluorescence shift between red (aggregates) and green (monomers) indicates changes in membrane potential.

(L) Quantification of the red/green fluorescence intensity ratio to assess ΔΨm changes.

(M) Mitochondrial reactive oxygen species (mtROS) were measured using MitoSOX™ Red fluorescence. HL-1 cells were subjected to HG conditions with or without shRNA/mtHsp70 treatment.

(N) Fluorescence intensity of mtROS was quantified using confocal microscopy and ImageJ software.

All data are presented as mean ± SD. In each group, six animals or six independent cell isolations were used. Each experiment was conducted with three replicates.

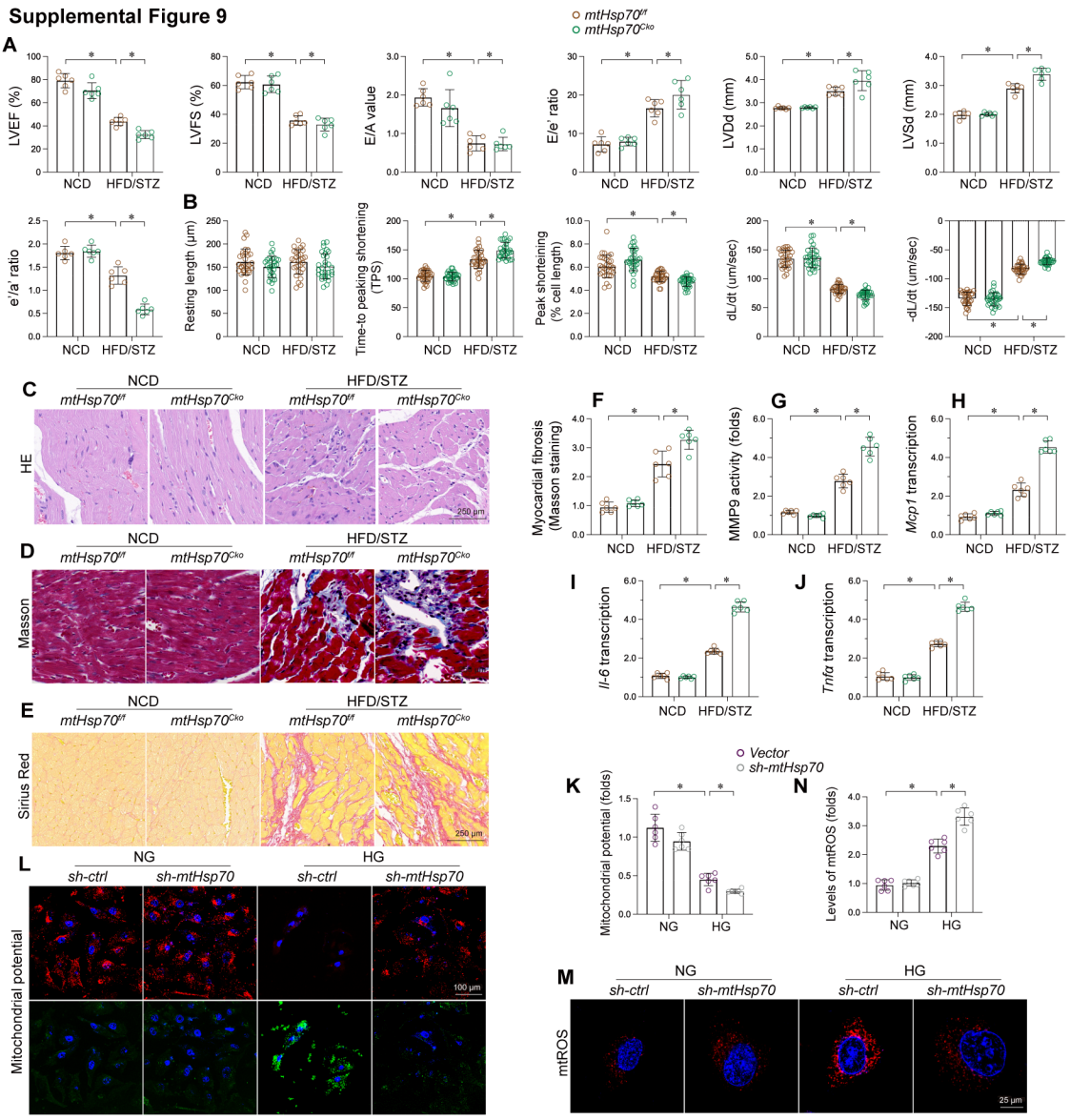

Supplemental Figure 10. Dusp15 deficiency contributes to hyperglycemia-mediated mtHsp70 phosphorylation.

To evaluate the phosphorylation of mtHsp70 at specific residues, HL-1 cells exposed to hyperglycemia were subjected to immunoprecipitation using specific antibodies raised against phosphorylated mtHsp70 at Thr116 (p-mtHsp70^{T116}) and Tyr118 (p-mtHsp70^{Y118}). Sodium orthovanadate (SO), a broad phosphatase inhibitor, was applied to determine the dependency of mtHsp70 dephosphorylation on Dusp15 phosphatase activity *in vitro*.

All data are presented as mean ± SD. In each group, six animals or six independent cell isolations were used. Each experiment was conducted with three replicates and the dots in each panel represent the outcomes of these replicate experiments.

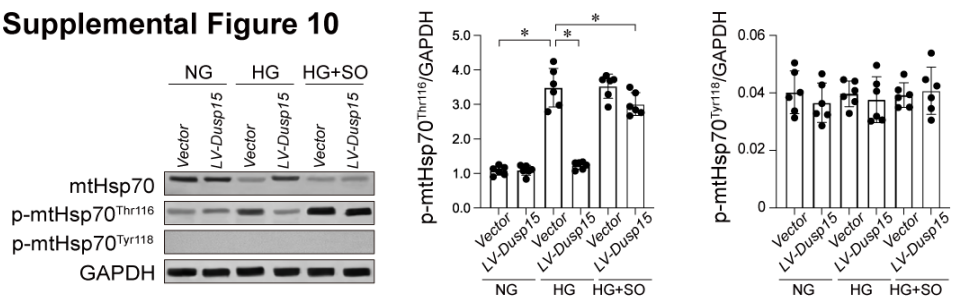

Supplemental Figure 11. mtHsp70 dephosphorylation preserves mitochondrial function and cardiomyocyte function during DCM. HL-1 cells were transfected with either wild-type mtHsp70, phosphorylation-defective mtHsp70^{T116A}, or phosphorylation-mimetic mtHsp70^{T116D} constructs before HG treatment.

(A-B) ΔΨm was assessed using JC-1 staining. Cells were incubated with JC-1 probe, and fluorescence was analyzed to evaluate ΔΨm changes under HG stress.

(C-D) mtROS levels were measured using MitoSOX Red staining. Cells were stained and visualized via confocal microscopy, with fluorescence intensity analyzed using ImageJ software.

(E) Cardiomyocyte viability was evaluated using an MTT assay after HG exposure.

(F-I) mito-UPR activity was assessed by analyzing transcriptional levels of genes related to mito-UPR. All data are presented as mean ± SD. In each group, six animals or six independent cell isolations were used. Each experiment was conducted with three replicates.

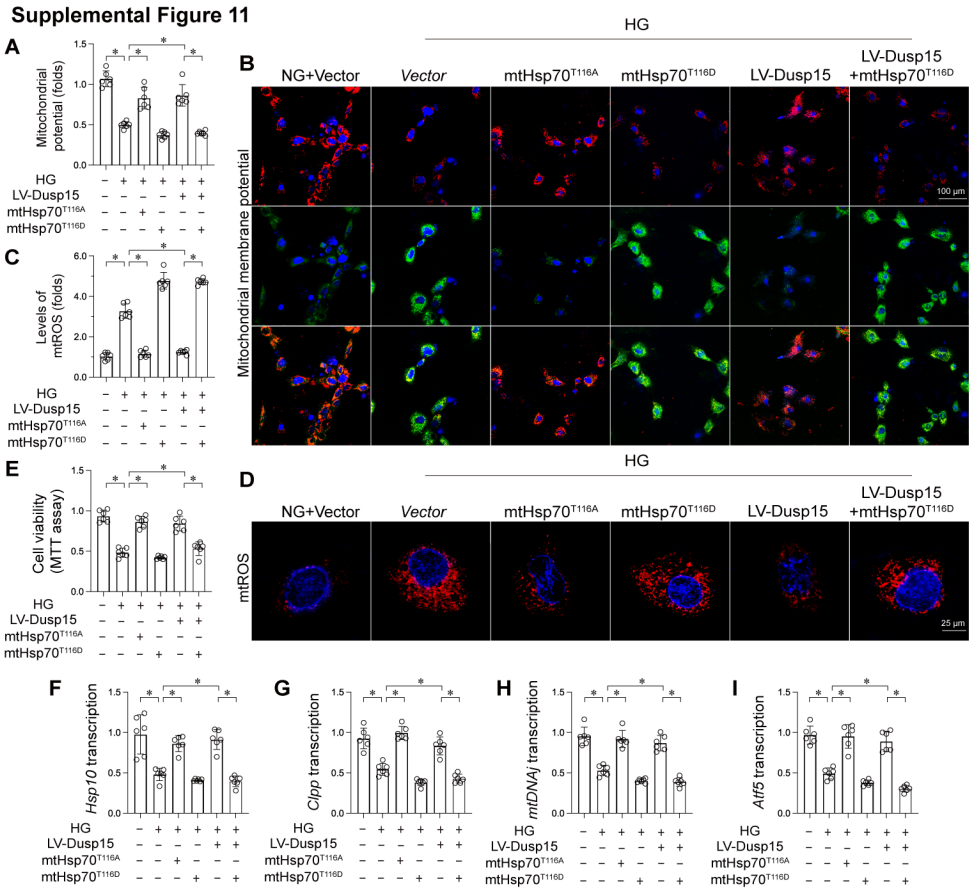

Supplemental Figure 12. Generation and validation of mtHsp70-T116A knock-in mouse.

(A-B) HE staining, Masson staining, Sirius red staining, TUNEL staining, and Nissl staining were performed to observe the histological alterations of kidney, liver and brain in WT, heterozygous *mtHsp70T116*$^{A/+}$ mice, and homozygous *mtHsp70T116*$^{A/A}$.

(C) The concentrations of BNP, TnT, Scr, BUN, AST and ALT in the serum were determined by ELISA. All data are presented as mean ± SD. In each group, six animals or six independent cell isolations were used. Each experiment was conducted with three replicates.

Supplemental Figure 12

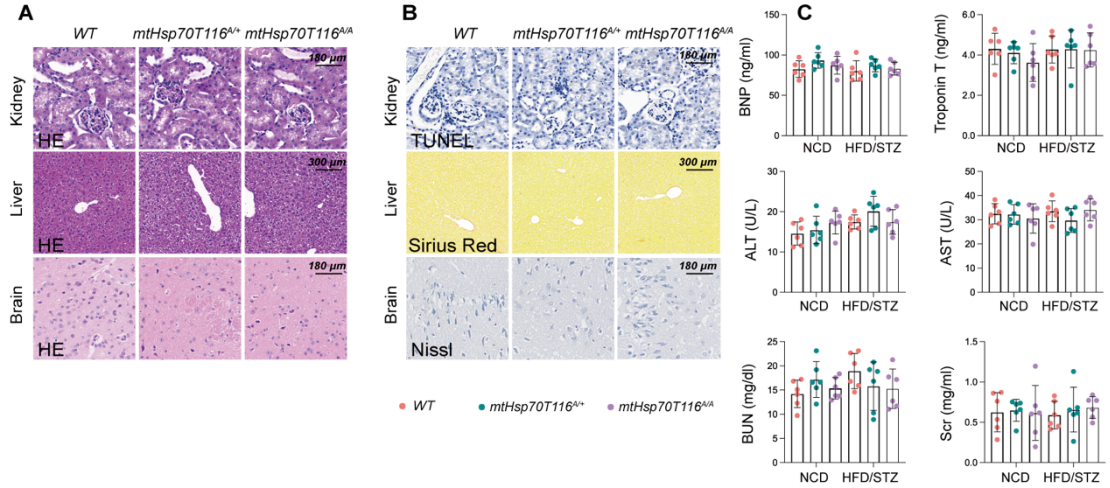

Supplemental Figure 13. The cardioprotective effects of DAPA requires Dusp15/mtHsp70 pathway. WT and cardiomyocyte-specific *Dusp15* knockout (*Dusp15*^{Cko}) mice were subjected to a high-fat diet (HFD) combined with low-dose streptozotocin (STZ) to induce a DCM model. Diabetic mice were treated with DAPA (10 mg/kg/day, oral administration) for 12 weeks. Vehicle-treated groups served as controls.

(A) Heart tissues from DAPA-treated and control mice were lysed using RIPA buffer. Proteins were separated by SDS-PAGE and immunoblotted using specific antibodies targeting Dusp15, mtHsp70, and phosphorylated mtHsp70 (Thr116).

(B-E) qPCR assay was used to evaluate the transcription of mito-UPR-related markers.

All data are presented as mean ± SD. In each group, six animals or six independent cell isolations were used. Each experiment was conducted with three replicates.

Supplemental Figure 13